Journal of Physical Science
Vol. 37(1), 21–41, 2026

Plasmonic Evaluation and Anticancer Potential of Gold Nanoparticles Synthesised via Sonochemical Route from Plum Peel Waste

Mohammed Ali Dheyab,[1,2*] Jia Hui Tang[1], Shaymaa Hussein Nowfal,[3,4]
Azlan Abdul Aziz,[1,2*] Pegah Moradi Khaniabadi,[5] Baharak Mehrdel,[6]
Mahmood S. Jameel[7] and Saleh T. Alanezi[8]

[1]School of Physics, Universiti Sains Malaysia, 11800 Pulau Pinang, Malaysia
[2]Nano-Biotechnology Research and Innovation (NanoBRI), Institute for Research in Molecular Medicine (INFORMM), Universiti Sains Malaysia, 11800 Pulau Pinang, Malaysia
[3]Medical Physics Department, College of Science, University of Warith Al-Anbiyaa, Karbala 56001, Iraq
[4]Medical physics department, College of Applied Medical Sciences, University of Kerbala, Karbala 56001, Iraq
[5]Community and Health Research Unit (CaHRU), School of Health and Social Care, University of Lincoln, Lincoln, LN5 7AY, UK
[6]Department of Radiology and Biomedical Imaging, University of California San Francisco, San Francisco, CA 94143, USA
[7]Pharmaceutical Design and Simulation Laboratory, School of Pharmaceutical Sciences, Universiti Sains Malaysia, 11800 Pulau Pinang, Malaysia
[8]Department of Physics, College of Science, Northern Border University, Arar P.O. Box 1321, Saudi Arabia

*Corresponding author: mdali@usm.my, lan@usm.my

Published online: 29 April 2026

To cite this article: Dheyab, M. A. et al. (2026). Plasmonic evaluation and anticancer potential of gold nanoparticles synthesised via sonochemical route from plum peel waste. *J. Phys. Sci.*, 37(1), 21–41. https://doi.org/10.21315/jps2026.37.1.2

To link this article: https://doi.org/10.21315/jps2026.37.1.2

ABSTRACT: The integration of sustainable nanomaterials with advanced optical functionalities is essential for the development of next-generation biomedical devices. This study reports the ultrasound-assisted green synthesis of plasmonic gold nanoparticles (AuNPs) using *Prunus salicina* (plum) peel extract a novel approach that valorises food waste for the production of high-value nanomaterials. The synthesised AuNPs were comprehensively characterised using UV–visible (UV-Vis) spectroscopy, X-ray diffraction (XRD), dynamic light scattering (DLS), field emission scanning electron microscopy (FESEM) and energy-dispersive X-ray spectroscopy (EDX). UV-Vis analysis revealed a distinct surface plasmon resonance (SPR) peak at 538 nm, confirming successful nanoparticle formation, with optical tunability influenced by sonication time. The AuNPs exhibited excellent stability (zeta potential: –34 mV) and a predominantly spherical morphology, with an average hydrodynamic size of 41 nm. FESEM confirmed their uniform distribution, while EDX validated the elemental composition. In addition, in vitro cytotoxicity studies using the MCF-7 human breast cancer cell line demonstrated dose-dependent anticancer activity, underscoring the biomedical potential

of the synthesised nanoparticles. This work establishes a green, rapid and scalable route for producing optically functional AuNPs with promising applications in plasmonic biosensing, photothermal therapy and other biomedical fields.

Keywords: gold nanoparticles, sonochemical synthesis, plum peel extract, green nanotechnology, anticancer activity

1. INTRODUCTION

Nanotechnology is a rapidly advancing field that enables the design of materials with distinctive physicochemical properties through precise control at the nanoscale.[1–4] Its interdisciplinary nature has opened new avenues for environmentally responsible innovations in medicine, energy, catalysis, antibacterial technologies and sensing, particularly through sustainable synthesis routes employing plant-derived compounds.[5–9] Among the wide range of nanomaterials, gold nanoparticles (AuNPs) have garnered considerable attention due to their size-dependent physicochemical and optical characteristics, especially localised SPR (LSPR), which is highly sensitive to variations in particle size, morphology and the surrounding dielectric medium.[10,11] These properties make AuNPs suitable for diverse applications including biosensing, photothermal therapy, catalysis, drug delivery and diagnostic imaging.[12–15] However, most conventional synthesis techniques employ chemical reducing agents such as sodium borohydride or trisodium citrate, which typically require elevated temperatures and generate environmentally hazardous by-products.[16–18] These drawbacks have prompted growing interest in eco-friendly, plant-mediated green synthesis approaches.

Green synthesis methods exploit phytochemicals such as flavonoids, phenolic acids and terpenoids, which act as both reducing and stabilising agents.[19–23] These compounds, naturally present in plant extracts, facilitate the formation of biocompatible and stable AuNPs under mild reaction conditions. Although more sustainable, these methods are often limited by extended reaction times, inadequate control over nanoparticle morphology, and batch-to-batch variability. To address these challenges, sonochemical methods have emerged as a promising complementary strategy. Sonochemistry utilises acoustic cavitation to accelerate nucleation and improve dispersion, leading to rapid synthesis and tunable nanoparticle characteristics.[24,25] The integration of sonochemistry with phytochemical-mediated reduction thus provides a synergistic pathway for fast, green and controllable AuNP production.

Several studies have investigated plant-mediated synthesis of AuNPs using sources such as *Carissa macrocarpa*, *halophytes*, *Croton caudatus* and *Kaempferia parviflora.*[26–29] However, many of these focus on whole plants or medicinal herbs, with limited emphasis on the valorisation of agro-industrial waste. This represents a significant research gap, particularly in light of the global shift towards circular economy

practices and sustainable material development. Recent examples highlight the multifunctionality of green-synthesised AuNPs, such as *Fagonia arabica*–mediated particles for sensing, photocatalysis and antibacterial activity and *Cyperus scariosus*–derived AuNPs serving as both colorimetric probes and antimicrobial agents.[30–31]

Compared with conventional plant-based synthesis methods, sonochemical-assisted techniques provide several advantages, including shorter reaction times (typically under 10 min), dynamic SPR tuning through adjustments in sonication time and amplitude, and improved colloidal stability. Nevertheless, few studies have explored the combination of sonochemical approaches with food waste as a reductant source. Moreover, while many reports on green synthesis speculate on biomedical potential, relatively few validate such claims with functional assays or provide insights into plasmonic tunability.

Food waste such as fruit peels constitutes an abundant yet underutilised resource, rich in polyphenolic compounds. In particular, *Prunus salicina* (plum) peel has been shown to contain ferulic acid, m-coumaric acid, quercetin and anthocyanins bioactive molecules that can act as reducing and capping agents in nanoparticle synthesis.[32–33] Exploiting this waste stream not only provides environmental and economic value but also supports global efforts to reduce agricultural residues in landfills. However, variations in biochemical composition due to source and seasonality present challenges for reproducibility and scalability, which warrant further investigation.

To address these gaps, this study proposes a rapid, environmentally friendly protocol for synthesising AuNPs by combining *Prunus salicina* peel extract with sonochemistry. Specifically, we examine how sonication time a dynamic synthesis parameter influences nanoparticle characteristics including SPR peak, particle size and colloidal stability. We hypothesise that the bioactive compounds in plum peel, when coupled with acoustic energy, will enable the controlled synthesis of stable, optically active AuNPs with biomedical potential. The objectives of this study are to: (1) evaluate the effects of sonication time on SPR tuning, particle size and surface charge, and (2) assess the cytotoxicity of the resulting nanoparticles against the MCF-7 breast cancer cell line as a model for biomedical applicability. Ultimately, this work aims to establish a scalable, waste-to-nanomaterial pathway that advances both sustainable nanotechnology and functional biomedical applications. It further contributes to the field of optical nanobiotechnology by presenting a highly scalable and environmentally conscious approach for plasmonic nanomaterial production from waste resources, while mapping the influence of dynamic synthesis parameters particularly sonication time on plasmonic, structural and biological properties.

2. MATERIALS AND METHODS

2.1 Materials

Five hundred grams of plum were obtained from a local supermarket on Penang Island, Malaysia. The plums were imported by Khaishen Trading Sdn. Bhd., Selangor, Malaysia, from South Africa. Chloroauric acid ($HAuCl_4{\cdot}4H_2O$) was purchased from Sigma-Aldrich, St. Louis, MO, USA. The MCF-7 cell line was obtained from the American Type Culture Collection (ATCC), Manassas, VA, USA. Dulbecco's Modified Eagle Medium (DMEM), penicillin, streptomycin, foetal bovine serum (FBS) and trypsin–ethylenediamine tetraacetic acid (trypsin–EDTA) were supplied by Gibco, Thermo Fisher Scientific, Waltham, MA, USA. 3-(4,5-Dimethylthiazol-2-yl)-2,5-diphenyltetrazolium bromide (MTT) was purchased from Fisher Scientific, Waltham, MA, USA. Dimethyl sulfoxide (DMSO) was obtained from Bio Basic Inc., Markham, Ontario, Canada.

2.2 *Prunus Salicina* Preparation and Extraction

The *Prunus salicina* peel was thoroughly washed with distilled water (DW) before the outer layer was carefully removed using a peeler to eliminate any surface contaminants. The peeled skin was then cut into smaller pieces, and 30 g of *Prunus salicina* peel were weighed for use in this study. The measured peel was transferred into a beaker containing 200 mL of DW and heated for 25 min on a magnetic stirrer equipped with a hot plate. The resulting extract was filtered through Whatman No. 1 filter paper to obtain a clear solution, which was subsequently stored at 4°C until further use.

2.3 Colloidal

In this study, a Vibra-Cell horn operating at a frequency of 20 kHz with a power output of 750 W was employed. Initially, 30 mL of a precursor solution containing $HAuCl_4$ at a concentration of 0.5 mM was subjected to sonication for 10 min at an ultrasonic frequency of 20 kHz and an amplitude (Amp) ranging from 25%–35%. The precursor solution was then treated with the dropwise addition of 3.5 mL of prepared plum peel extract. Sonication continued for a further minute at 35% amplitude until the solution changed colour from yellow to light purple, indicating the onset of nucleation. After an additional minute of sonication at 35% amplitude, the reaction mixture reached a stable purple colour. During this process,

5 mL samples were collected at different time intervals, beginning at the 1st min and continuing until a consistent purple colour was achieved in the 5th min. For subsequent analyses, the collected samples were stored at 4°C. Figure 1 illustrates the synthetic steps, from sample preparation to the formation of AuNPs.

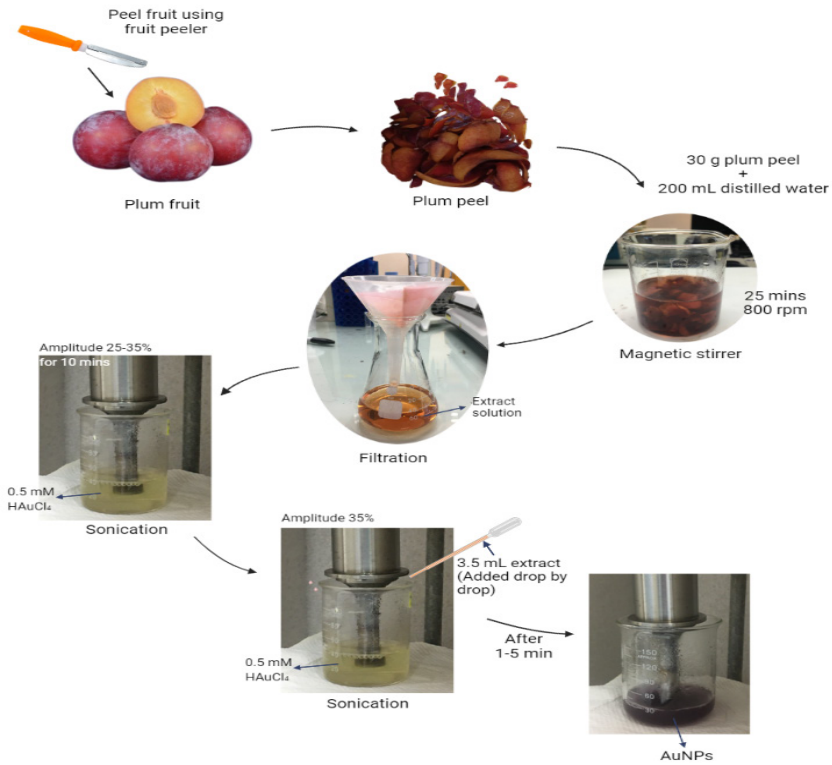

Figure 1: The synthetic process showing the steps from preparation to AuNPs production.

2.4 Characterisation of Green-synthesised AuNPs

The AuNPs colloidal solution was characterised using several analytical techniques. X-ray diffraction (XRD) Bruker D8 Advance, Bruker, Billerica, MA, USA) was used to analyse crystallinity. Dynamic Light Scattering (DLS) (Zetasizer Nano ZS, Malvern Panalytical, Malvern, UK) was employed to determine hydrodynamic size and zeta potential (ZP). Ultraviolet–visible spectrophotometry (UV-Vis; UV-

3600, Shimadzu, Kyoto, Japan) was used to obtain absorption spectra. Morphology and grain size were evaluated using Field Emission Scanning Electron Microscopy (FESEM) (Nova NanoSEM 450, FEI, Hillsboro, OR, USA). FESEM images were processed with ImageJ software (NIH, Bethesda, MD, USA) for particle size determination, and OriginPro (OriginLab, Northampton, MA, USA) was used to construct size distribution histograms. Elemental composition was examined using an energy-dispersive X-ray (EDX; X-Max, Oxford Instruments, Abingdon, UK) system integrated with the FESEM.

2.5 Assessment of the Anticancer Potential of AuNPs Colloidal

The anticancer properties of the AuNPs were evaluated using the MTT assay, a widely employed in vitro method for assessing cell proliferation, metabolic activity and the effects of nanoparticles on DNA.[34] MCF-7 cells were cultured at 37°C in a humidified atmosphere containing 5% carbon dioxide (CO_2) and 95% relative humidity in DMEM supplemented with 10% FBS and 1% penicillin/streptomycin. After 24 h, the cells were harvested using trypsin and seeded into 96-well plates at a density of 5×10^3 cells per well in 100 µL of complete DMEM, followed by incubation for another 24 h under the same conditions.

Subsequently, the cells were treated with 100 µL of DMEM containing six different concentrations of AuNPs (0, 26, 39, 59, 89 and 133 µg/mL) and incubated for 24 h. Each concentration was tested in triplicate. Thereafter, 30 µL of MTT solution (25 mg/10 mL in PBS) was added to each well, and the plates were incubated for a further 4 h at 37°C in 5% CO_2. The medium was then carefully removed, and 100 µL of DMSO was added to each well to dissolve the formazan crystals. The plates were incubated for 5 min, and absorbance was measured at 570 nm using a microplate reader (Thermo Scientific Multiskan Spectrum). Cell viability was calculated using the following Equation (1):[35]

$$Cell\ Viability\ (\%) = \frac{Sample\ A}{Control\ A} \times 100 \quad (1)$$

Where, *Sample A.* and *Control A.* denote the absorbance values of the treated and control cells, respectively.

3. RESULTS AND DISCUSSION

3.1 Crystalline Structure of Synthesised AuNPs

XRD is a non-destructive technique widely used to characterise the crystallinity of metallic nanoparticles.[36,37] It can also be employed to estimate particle size using the Debye–Scherrer equation (Equation [2]):[38]

$$D = \frac{Kl}{b \cos q} \tag{2}$$

Where, D is the crystallite size, K is the Scherrer constant (0.9), l is the wavelength of the X-ray radiation (0.14924 nm), b is Full Width Half Maximum (FWHM), while q is angle of diffraction (half of the Bragg angle). As shown in Figure 2, five prominent XRD peaks were observed at 2θ values of 35.95°, 41.36°, 64.60°, 76.47° and 81.07°, corresponding to the (111), (200), (220), (311) and (222) crystallographic planes of face-centred cubic (FCC) gold crystals, respectively.[39] Based on Equation (2), the average crystallite size of the AuNPs was calculated to be 9.67 nm.

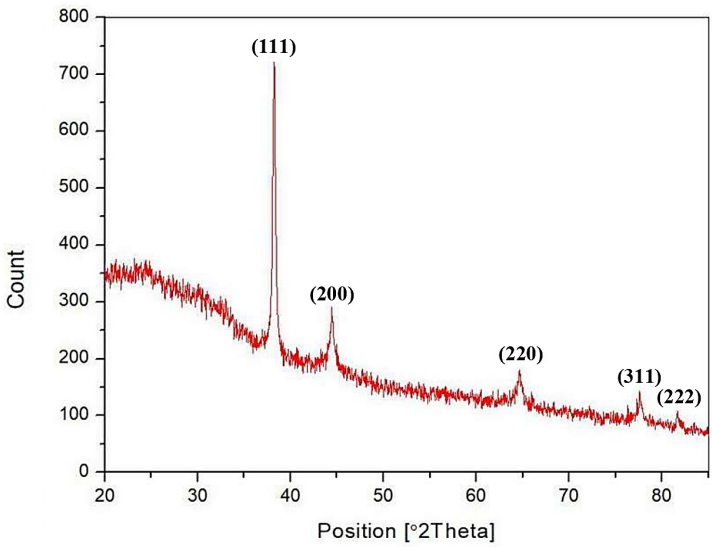

Figure 2: The XRD pattern of AuNPs colloidal synthesised using *Prunus salicina* peel extract.

3.2 Optical Properties and Visual Analysis of Green-synthesised AuNPs Colloidal

As shown in Figure 3(a), the colour of the plum peel extract changed from light yellow to purple when mixed with 0.5 mM $HAuCl_4$. This colour change confirmed the successful synthesis of AuNPs and is consistent with the reported colour transformation of AuNPs synthesised from *Prunus persica* peels by Patra et al.[40] The solution turned light purple within just 1 min of sonication, indicating the rapid onset of AuNP formation a markedly shorter time frame than those reported in earlier studies.[20] The synthesis proceeded in a fast and straightforward manner under ultrasonic irradiation. At a frequency of 20 kHz, ultrasonic waves generate regions of high temperature and pressure in the reaction medium.[41] This induces acoustic cavitation, leading to the formation, expansion and collapse of microbubbles.[42] The collapse releases kinetic energy that promotes rapid mixing between Au^{3+} ions and bioactive radicals present in *Prunus salicina* extract.[43] Through this sonochemical reaction mechanism, Au^{3+} ions are reduced to Au^0. In addition, plum peel is rich in phenolic compounds such as ferulic acid, m-coumaric acid and quercetin, as well as flavonoids, anthocyanins and amines, all of which can act as reducing agents to facilitate nanoparticle synthesis.[44,45]

UV-Vis spectroscopy was employed as a preliminary tool to confirm the synthesis of AuNPs and study their absorption properties. The observed absorption spectra can be explained by SPR, which arises from the strong interaction between delocalised electrons on the nanoparticle surface and incident light.[46] The absorbance of five samples was measured in the range of 400 nm–700 nm, with DW serving as the reference. As shown in Figure 3(b), the highest absorbance peak appeared at 538 nm for a sonication time of 5 min. This peak lies within the characteristic AuNP range of 500 nm–550 nm.[37] supporting the successful formation of nanoparticles. Furthermore, the absence of a peak in the spectra of the extract and $HAuCl_4$ alone, followed by its appearance after sonication, provides further evidence of nanoparticle synthesis. Notably, the SPR peaks exhibited a slight blue shift, shifting from 542 nm–538 nm as sonication time increased from 1 min–5 min. Since SPR is highly sensitive to nanoparticle size, shape, interparticle distance and the dielectric constant of the surrounding medium, this shift suggests subtle modifications in the colloidal environment and particle interactions during synthesis.[47]

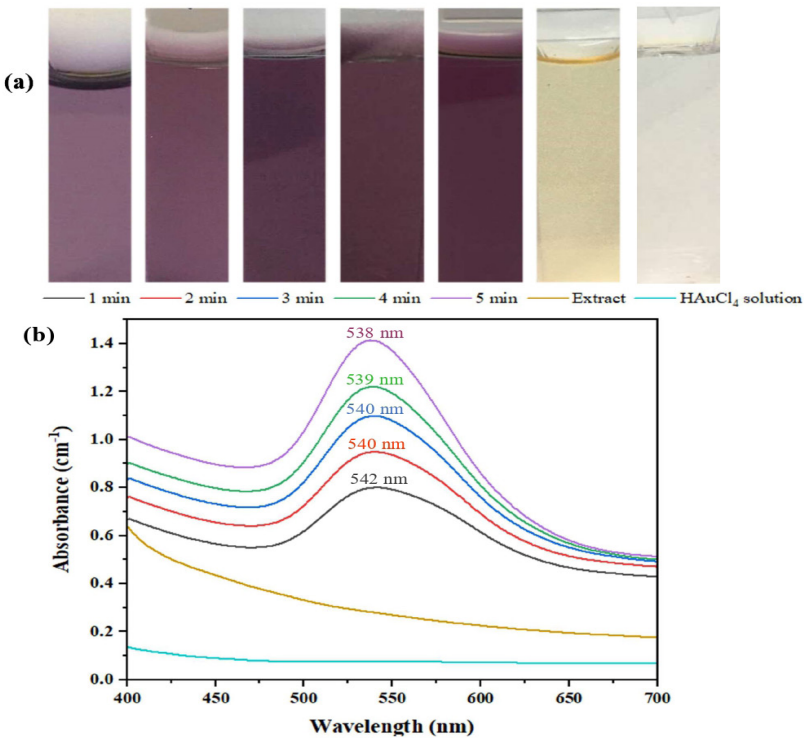

Figure 3: (a) Colour change observation of AuNPs colloidal at various time intervals of the synthesis NPs and (b) UV-vis analysis of synthesised AuNPs colloidal solution mediated by sonication of 1 min–5 min.

3.3 Size and Morphology of Synthesised Green AuNPs

The size and morphology of the prepared samples were examined using FESEM. Figure 4(a) shows the FESEM images of AuNPs, which were predominantly spherical. The size distribution histogram indicated an average particle size of 35.1 nm. In comparison, the hydrodynamic size determined by DLS (Figure 5) was 40 nm. The observed variation between FESEM and DLS results may be attributed to the diverse bio-compounds present in the plant extract, which act as reducing agents for Au^{3+} ions. These bio-compounds differ in their composition and reactivity, thereby contributing to variability in nanoparticle size. In contrast, nanoparticles synthesised using chemical reducing agents typically exhibit greater uniformity, as the reduction process is more controlled, often producing particles with consistent sizes and shapes.[48]

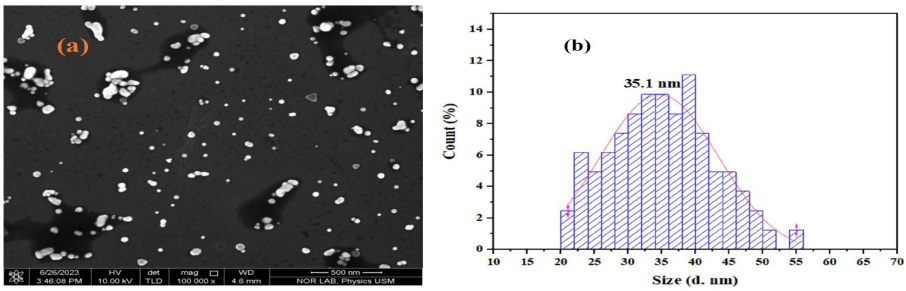

Figure 4: (a) FESEM image of AuNPs and (b) Size distribution histogram of sonochemically synthesised AuNPs.

3.4 Hydrodynamic Size and ZP of Green-synthesised AuNPs Colloidal

Hydrodynamic size and ZP measurements were carried out using DLS. The hydrodynamic diameter obtained by DLS is typically larger than the size measured by Transmission electron microscopy (TEM), owing to the presence of bio-organic compounds encapsulating the AuNPs. As shown in Figure 5, the average hydrodynamic size of AuNPs after 5 min of sonication was 41 nm, with values ranging between 37.36 nm and 51.78 nm. An increasing trend in particle size was observed between one and 4 min of sonication. This increase can be attributed to nucleation and particle growth occurring during the synthesis process.[15] Nucleation was confirmed by the visible colour change of the precursor solution from light yellow to colourless, indicating the initial formation of small nanoparticles. With continued sonication from one to 4 min, the AuNPs grew further, resulting in the development of a colloidal solution and, at times, the agglomeration of particles.

At 5 min, however, the data revealed a reduction in hydrodynamic size, indicating the dispersion of agglomerated AuNPs. This phenomenon occurs because the large aggregates formed at 4 min are broken apart under continued sonication, leading to electrostatic repulsion. The nanoparticles formed at this stage exhibited a weak surface charge that promoted their redispersion into smaller, more stable forms. Overall, these results suggest that short sonication times can initially increase hydrodynamic size through growth and agglomeration, but extended sonication facilitates the dispersion of aggregates, yielding smaller and more stable colloidal nanoparticles.

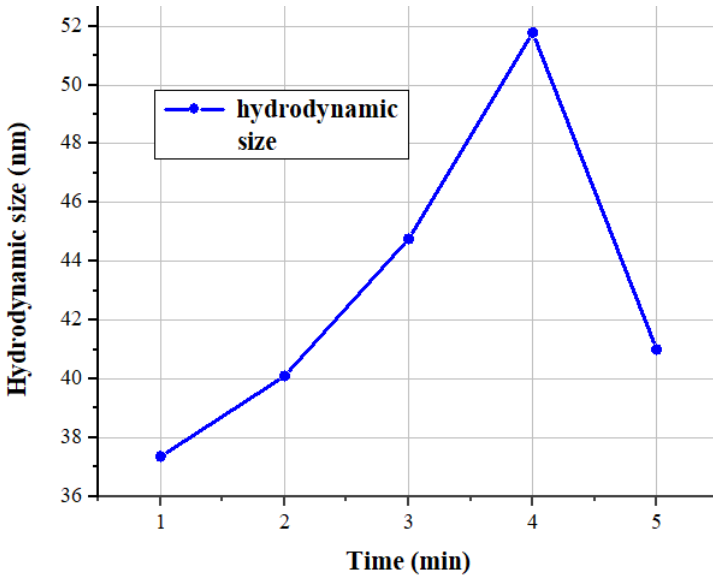

Figure 5: Hydrodynamic size of AuNPs synthesised by *Prunus salicina* (1 min–5 min).

ZP reflects the electrostatic potential at the ionic surface of nanoparticles. A nanoparticle suspension is generally considered stable if the ZP value exceeds +30 mV or is lower than –30 mV.[49] In this study, the ZP values recorded at 1 min, 2 min, 3 min, 4 min and 5 min of sonication were –24.6 mV, –29.4 mV, –26.2 mV, –27.5 mV and –34 mV, respectively. The negative ZP values indicate that the AuNPs were surrounded by negatively charged bio-compounds from the plum peel extract. These compounds provide steric and electrostatic stabilisation, preventing particle agglomeration and thereby enhancing colloidal stability.[15] With increasing sonication time, the ZP values showed a downward trend, particularly between 3 min and 5 min, where the potential decreased from –26.2 mV– –34 mV. This gradual depletion reflects stronger electrostatic repulsion among the nanoparticles, leading to enhanced stability. The AuNPs synthesised at 5 min exhibited the highest stability, with a ZP of –34 mV.

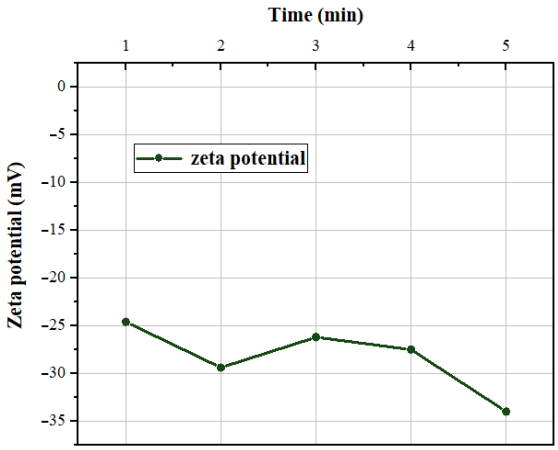

Figure 6: ZP results of AuNPs synthesised using plum peel food waste (1–5 min).

As the hydrodynamic size measurements indicated an overall increase in particle size with longer sonication times, particle size alone cannot explain the observed blueshift in the SPR peak (Figure 3[b]). According to Mie theory, a decrease in nanoparticle size results in a higher surface-to-volume ratio, making the SPR position highly sensitive to environmental factors such as changes in the refractive index of the medium or the formation of organic shells on the nanoparticle surface.[50] In this study, the elemental composition of the plum peel extract likely varied with sonication time, altering both the type and quantity of bio-compounds adhering to the AuNP surfaces. Such variations in surface chemistry and surrounding medium properties are plausible explanations for the blueshift observed in the SPR peaks.

3.5 Elemental Composition of Green-synthesised AuNPs

The EDX spectrum of the AuNPs colloidal sample prepared after 2 min of sonication confirmed the successful formation of AuNPs. As shown in Figure 7, the elemental composition indicated that gold accounted for 14.12% by weight. The spectrum also displayed the presence of silicon (Si), originating from the substrate used in preparing the thin film sample. In addition, non-metallic peaks corresponding to carbon (C) and oxygen (O) were detected, which can be attributed to the bio-compounds present in the plum peel extract that acted as reducing and stabilising agents.[51]

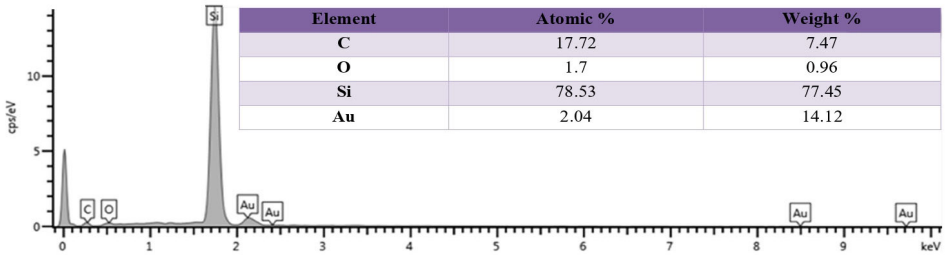

Element	Atomic %	Weight %
C	17.72	7.47
O	1.7	0.96
Si	78.53	77.45
Au	2.04	14.12

Figure 7: EDX elemental analysis of AuNPs synthesised using plum peel extract (2 min).

3.6 Anticancer Activity of Green-synthesised AuNPs in MCF-7 Cells

The cytotoxic activity of green-synthesised AuNPs against MCF-7 breast cancer cells was assessed using the MTT assay. Cells were treated with different AuNP concentrations (26 μg/mL, 39 μg/mL, 59 μg/mL, 89 μg/mL and 133 μg/mL) for 24 h, with each concentration tested in triplicate. As shown in Figure 8, cell viability decreased in a clear dose-dependent manner, demonstrating the cytotoxic potential of the nanoparticles. In contrast, the control group of untreated MCF-7 cells retained high viability, confirming that the culture conditions did not affect baseline cellular function. Cells exposed to increasing AuNP concentrations exhibited reduced viability, underscoring the effectiveness of these nanoparticles in inducing cell death.[52] Several mechanisms may explain the anticancer effects of AuNPs. First, nanoparticles can stimulate the generation of reactive oxygen species (ROS), causing oxidative stress that damages DNA, proteins and lipids, ultimately initiating apoptosis.[53] Secondly, AuNPs may accumulate within mitochondria, impairing their function, depleting cellular energy and releasing pro-apoptotic factors that further promote programmed cell death.[54] Additionally, their interaction with the plasma membrane may disrupt its integrity, increasing permeability and leading to cell lysis.[55] Together, these mechanisms activate apoptotic pathways, thereby enabling targeted elimination of cancer cells a desirable feature for anticancer therapy.[56]

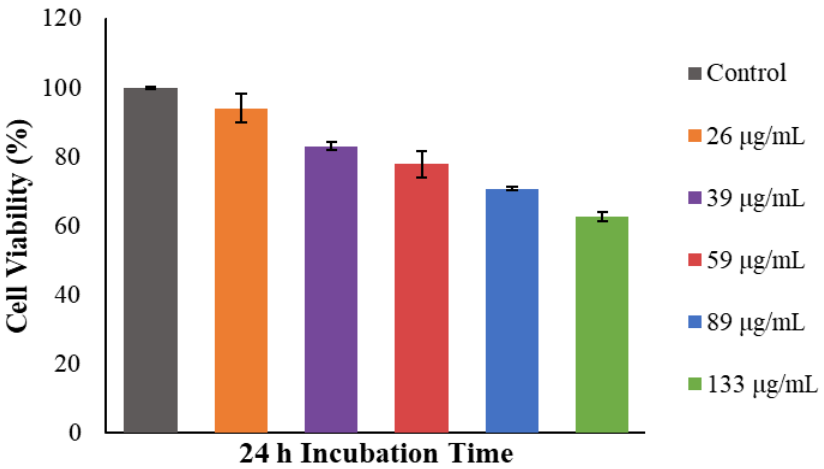

Figure 8: Cell viability of MCF-7 cells when exposed to different concentrations of AuNPs (26–133 µg/mL) at 24 h of incubation time.

It is also noteworthy that these nanoparticles were synthesised using *Prunus salicina* peel extract as a natural reducing agent, emphasising both the sustainability and eco-friendly nature of the approach. This aligns with the principles of green nanotechnology and provides a promising alternative to conventional chemical synthesis for biomedical applications.[57] Beyond their cytotoxicity towards MCF-7 cells, the physicochemical features of the nanoparticles small size (~35 nm), strongly negative ZP (–34 mV) and stable colloidal nature suggest their potential utility in broader biomedical contexts.[58] The phytochemical capping agents from plum peel, particularly flavonoids and phenolics, may further enhance bioactivity by promoting cellular uptake and modulating oxidative stress responses.[59,60] Although mechanistic assays such as ROS quantification or mitochondrial potential analysis were not performed in this work, the observed dose-dependent cytotoxicity, supported by previously reported mechanisms, indicates a multifactorial mode of action. In addition to cancer therapy, these properties may also be harnessed for photothermal therapy, drug delivery, biosensing and antimicrobial strategies. Future studies are planned to validate these mechanisms in different cell models. Finally, Table 1 provides a comparative summary of our sonochemically synthesised AuNPs against other reported green-synthesised systems, highlighting distinctions in particle size, ZP, biological activity and novelty to contextualise the advantages of the present study.

Table 1: Comparative summary of selected green synthesis methods for AuNPs.

Plant source	Synthesis method	Morphology/ size (nm)	Zeta potential	Application	Novelty	Refs
Moringa oleifera flowers	Aqueous extract mixed with 1 mM $HAuCl_4$ at room temperature	Spherical, triangular, hexagonal; 3–5 nm (TEM), ~203 nm (DLS)	–14.1 mV	Anticancer (A549), catalytic (4-NP & 4-NA)	Dual function: cytotoxic to cancer cells and active in wastewater degradation; green and scalable	[61]
Pineapple and *passion fruit peels*	Aqueous extract with dropwise $HAuCl_4$ addition at room temp	Pi-AuNPs: 20.71 ± 7.44 nm (spherical); Pa-AuNPs: 18.68 ± 5.55 nm (spherical)	Pi-AuNPs: –19.47 mV; Pa-AuNPs: –25.33 mV	Non-toxic in MCF-7 and Vero cells up to 400 µg/ mL	Demonstrated biocompatible AuNPs from food waste with no cytotoxicity and good stability	[62]
Grape-pomace waste (seeds + skins + stems)	One-pot, room temp reduction of $HAuCl_4$ with raw aqueous pomace extract	~30 nm polyhedral AuNP cores	–40	Antioxidant & waste-pomace reused to adsorb antibiotics	First "zero-waste" loop: same pomace stream makes AuNPs and becomes a pollutant adsorbent	[63]
Avocado (*Persea americana*) seed extract	80°C, 30 min extract-mediated reduction of $HAuCl_4$	~14 nm mostly spherical (TEM)	–24	Antioxidant, anticancer (PC-3, Caco-2), recyclable 4-NP catalyst	First to up-cycle avocado seeds into AuNPs combining bio-, anticancer, and catalytic functions	[64]
Garcinia kola fruit pulp	Mix 1 mL aqueous pulp extract with 1 mM $HAuCl_4$ (1 : 4 v/v), stir 5 h at room T, pH 7 (violet AuNPs after 48 h)	Spherical 18 – 38 nm (avg ≈ 28 nm, TEM)	…….	Antibacterial activity against *E. coli*, *P. aeruginosa*, *B. cereus*, *S. aureus*	First report of eco-friendly AuNPs from G. kola pulp with confirmed antibacterial potency	[65]
Plum (Prunus salicina) peel waste	20 kHz sonochemical, 0.5 mM $HAuCl_4$ + peel extract, colour change in ≤ 5 min	~35 nm spherical (TEM); 41 nm hydrodynamic	–34	Tunable SPR (538 nm) & dose-dependent cytotoxicity vs. MCF-7 cells	First report pairing sonochemistry with plum-waste phytochemicals for sub-5-min AuNP fabrication; SPR position controllable by sonication time; demonstrates anticancer efficacy while valorising food waste	Present study

4. CONCLUSION

This study demonstrated a green, sonochemically assisted method for synthesising AuNPs using *Prunus salicina* (plum) peel extract, an abundant agricultural waste material. The resulting AuNPs exhibited distinct plasmonic behaviour, with a sharp UV-Vis absorbance peak at 538 nm confirming their LSPR characteristics. XRD confirmed their crystalline structure, while DLS and FESEM revealed average particle sizes of 41 nm and 35.1 nm, respectively, with predominantly spherical shapes and occasional irregular or triangular morphologies. ZP analysis (–34 mV) indicated high colloidal stability, and EDX verified the elemental composition, including gold alongside bio-organic components from the extract. Importantly, the biosynthesised AuNPs displayed marked dose-dependent cytotoxicity against MCF-7 breast cancer cells, highlighting their potential as anticancer agents. Beyond their biological activity, this work establishes a scalable and eco-friendly pathway for converting fruit peel waste into high-value optical nanomaterials. The findings further demonstrate that sonication time acts as a tunable parameter for controlling SPR properties and nanoparticle stability, underscoring its significance in food-waste-derived AuNP synthesis. Future studies will extend this work by exploring additional biomedical and technological applications, including antimicrobial activity, photothermal therapy, and integration into optical diagnostic platforms.

5. ACKNOWLEDGEMENTS

This work was supported by a Universiti Sains Malaysia, Bridging Grant with Project No: R501-LR-RND003-0000002097-0000.

6. REFERENCES

1. Harb, N. H. et al. (2024). Preparation and characterisation of CdO@Au nanoparticles by hybrid system using laser ablation and plasma jet methods for cytotoxicity against rat embryonic fibroblast cell line. *J. Phys. Sci.*, 35(3), 17–25. https://doi.org/10.21315/jps2024.35.3.2
2. Dheyab, M. A. et al. (2021). Focused role of nanoparticles against COVID-19: Diagnosis and treatment. *Photodiagn. Photodyn. Ther.*, 34, 102287. https://doi.org/10.1016/j.pdpdt.2021.102287
3. Dheyab, M. A. et al. (2021). Recent advances in synthesis, medical applications and challenges for gold-coated iron oxide: Comprehensive study. *Nanomater.*, 11(8), 2147. https://doi.org/10.3390/nano11082147
4. Nowfal, S. H. et al. (2025). Design and decorated gold nanoparticles over the Arabic gum-chitosan hydrogel polymers as a novel catalyst for Sonogashira coupling reactions. *J. Organomet. Chem.*, 1038, 123762. https://doi.org/10.1016/j.jorganchem.2025.123762

5. Zafar, Z. et al. (2025). Tribological analysis of rabinowitsch fluid in peristaltic flow with gold nanoparticle suspension. *Tribol. Int.*, 110730. https://doi.org/10.1016/j.triboint.2025.110730
6. Ali, A. B. et al. (2025). Bio-supported of gold nanoparticles over magnetic nanoparticles: Synthesis, characterization and evaluation its catalytic activity for one-pot preparation of pyrano [2,3-d] pyrimidines. *J. Organomet. Chem.*, 123759. https://doi.org/10.1016/j.jorganchem.2025.123759
7. Abbas, A. et al. (2023). Growth of diazonium-functionalized ZnO nanoflakes on flexible carbon cloth for electrochemical sensing of acetone in the liquid phase. *RSC Adv.*, 13(17), 11537–11545. https://doi.org/10.1039/D3RA01268A
8. Jameel, M. S., Aziz, A. A. & Dheyab, M. A. (2021). Impacts of various solvents in ultrasonic irradiation and green synthesis of platinum nanoparticle. *Inorg. Chem. Commun.*, 128, 108565. https://doi.org/10.1016/j.inoche.2021.10856
9. Owaid, M. N. et al. (2022). Mycogenic fabrication of silver nanoparticles using Picoa, Pezizales, characterization and their antifungal activity. *Environ. Nanotechnol. Monit. Manag.*, 17, 100612. https://doi.org/10.1016/j.enmm.2021.100612
10. Dheyab, M. A. et al. (2023). Comparative analysis of stable gold nanoparticles synthesized using sonochemical and reduction methods for antibacterial activity. *Molecules*, 28(9), 3931. https://doi.org/10.3390/molecules28093931
11. Mehrdel, B. et al. (2020). Identifying metal nanoparticle size effect on sensing common human plasma protein by counting the sensitivity of optical absorption spectra damping. *Plasmonics*, 15, 123–133. https://doi.org/10.1007/s11468-019-01007-7
12. Chen, H. et al. (2024). Colorimetric biosensing assays based on gold nanoparticles functionalized/combined with non-antibody recognition elements. *TrAC Trends Anal. Chem.*, 117654. https://doi.org/10.1016/j.trac.2024.117654
13. Ferreira-Gonçalves, T. et al. (2024). Rational approach to design gold nanoparticles for photothermal therapy: The effect of gold salt on physicochemical, optical and biological properties. *Int. J. Pharm.*, 650, 123659. https://doi.org/10.1016/j.ijpharm.2023.123659
14. He, K. et al. (2024). Renal-clearable luminescent gold nanoparticles incorporating active and bio-orthogonal tumor-targeting for drug delivery and controlled release. *Nano Today*, 56, 102245. https://doi.org/10.1016/j.nantod.2024.102245
15. Dheyab, M. A., et al. (2021). Sonochemical-assisted synthesis of highly stable gold nanoparticles catalyst for decoloration of methylene blue dye. *Inorg. Chem. Commun.*, 127, 108551. https://doi.org/10.1016/j.inoche.2021.108551
16. Ali, A. B. et al. (2025). Design and synthesis of magnetic chitosan-supported gold nanoparticles and evaluating its usage in the Suzuki-Miyaura coupling reactions. *J. Organomet. Chem.*, 123677. https://doi.org/10.1016/j.jorganchem.2025.123677
17. Dheyab, M. A. et al. (2020). Rapid sonochemically-assisted synthesis of highly stable gold nanoparticles as computed tomography contrast agents. *Appl. Sci.*, 10(20), 7020. https://doi.org/10.3390/app10207020
18. Roth, J. et al. (2025). Post-synthetic modification of a MOF via continuous flow methods for gold e-waste recycling. *ChemSusChem*, 18(5), e202401642. https://doi.org/10.1002/cssc.202401642

19. Dheyab, M. A. et al. (2024). Green synthesis of gold nanoparticles and their emerging applications in cancer imaging and therapy: A review. *Rev. Inorg. Chem*. https://doi.org/10.1515/revic-2024-0048
20. Dheyab, M. A. et al. (2024). Turning food waste-derived ultrasmall gold nanoparticles as a photothermal agent for breast cancer cell eradication. *Inorg. Chem. Commun.*, 169, 113030. https://doi.org/10.1016/j.inoche.2024.113030
21. Rabeea, M. A. et al. (2021). Phytosynthesis of *Prosopis farcta* fruit-gold nanoparticles using infrared and thermal devices and their catalytic efficacy. *Inorg. Chem. Commun.*, 133, 108931. https://doi.org/10.1016/j.inoche.2021.10893
22. Khan, A. W. et al. (2024). Sunlight-assisted green synthesis of gold nanocubes using horsetail leaf extract: A highly selective colorimetric sensor for Pb^{2+}, photocatalytic and antimicrobial agent. *J. Environ. Chem. Eng.*, 12(3), 112576. https://doi.org/10.1016/j.jece.2024.112576
23. Al-Mafarjy, S. S. et al. (2024). Green synthesis of gold nanoparticles from *Coleus scutellarioides* (L.) Benth leaves and assessment of anticancer and antioxidant properties. *Inorg. Chem. Commun.*, 161, 112052. https://doi.org/10.1016/j.inoche.2024.112052
24. Ashassi-Sorkhabi, H. et al. (2015). Synthesis of Au nanoparticles by thermal, sonochemical and electrochemical methods: Optimisation and characterization. *Phys. Chem. Res.*, 3(1), 24–34. https://doi.org/10.22036/pcr.2015.7311
25. Dheyab, M. A. et al. (2021). Distinct advantages of using sonochemical over laser ablation methods for a rapid-high quality gold nanoparticles production. *Mater. Res. Express*, 8(1), 015009. https://doi.org/10.1088/2053-1591/abd5a4
26. Siddique, A. B. et al. (2025). *Carissa macrocarpa* extract based greenly synthesized AuNPs: A sustainable approach for lead ion detection, azo dye degradation, and antimicrobial applications. *Water Air Soil Pollut.*, 236(6), 1–22. https://doi.org/10.1007/s11270-025-08014-x
27. Hosny, M. et al. (2021). Comparative study on the potentialities of two halophytic species in the green synthesis of gold nanoparticles and their anticancer, antioxidant and catalytic efficiencies. *Adv. Powder Technol.*, 32(9), 3220–3233. https://doi.org/10.1016/j.apt.2021.07.008
28. Kumar, P. V., Kala, S. M. J. & Prakash, K. (2019). Green synthesis of gold nanoparticles using *Croton caudatus* Geisel leaf extract and their biological studies. *Mater. Lett.*, 236, 19–22. https://doi.org/10.1016/j.matlet.2018.10.025
29. Varghese, B. A. et al. (2021). Green synthesis of gold nanoparticles using *Kaempferia parviflora* rhizome extract and their characterization and application as an antimicrobial, antioxidant and catalytic degradation agent. *J. Taiwan Inst. Chem. Eng.*, 126, 166–172. https://doi.org/10.1016/j.jtice.2021.07.016
30. Shah, A. et al. (2024). *Fagonia arabica* extract-stabilized gold nanoparticles as a highly selective colorimetric nanoprobe for Cd^{2+} detection and as a potential photocatalytic and antibacterial agent. *Surf. Interfaces*, 51, 104556. https://doi.org/10.1016/j.surfin.2024.104556
31. Ejaz, A. et al. (2024). *Cyperus scariosus* extract based greenly synthesized gold nanoparticles as colorimetric nanoprobe for Ni^{2+} detection and as antibacterial and photocatalytic agent. *J. Mol. Liq.*, 393, 123622. https://doi.org/10.1016/j.molliq.2023.123622

32. Jawad, M. et al. (2022). Determination of phenolic compounds and bioactive potential of plum (*Prunus salicina*) peel extract obtained by ultrasound-assisted extraction. *Biomed. Res. Int.*, 2022(1), 7787958. https://doi.org/10.1155/2022/7787958
33. Basanta, M. F. et al. (2016). Antioxidant Japanese plum (*Prunus salicina*) microparticles with potential for food preservation. *J. Funct. Foods*, 24, 287–296. https://doi.org/10.1016/j.jff.2016.04.015
34. Kus-Liśkiewicz, M., Fickers, P. & Ben Tahar, I. (2021). Biocompatibility and cytotoxicity of gold nanoparticles: Recent advances in methodologies and regulations. *Int. J. Mol. Sci.*, 22(20), 10952. https://doi.org/10.3390/ijms222010952
35. Li, S. et al. (2021). Green synthesis of gold nanoparticles using aqueous extract of *Mentha longifolia* leaf and investigation of its anti-human breast carcinoma properties in the in vitro condition. *Arab. J. Chem.*, 14(2), 102931. https://doi.org/10.1016/j.arabjc.2020.102931
36. Akintelu, S. A., Yao, B. & Folorunso, A. S. (2021). Bioremediation and pharmacological applications of gold nanoparticles synthesized from plant materials. *Heliyon*, 7(3), e06591. https://doi.org/10.1016/j.heliyon.2021.e06591
37. Saravanan, A. et al. (2021). A review on biosynthesis of metal nanoparticles and its environmental applications. *Chemosphere*, 264, 128580. https://doi.org/10.1016/j.chemosphere.2020.128580
38. AbdelRahim, K. et al. (2017). Extracellular biosynthesis of silver nanoparticles using *Rhizopus stolonifer*. *Saudi J. Biol. Sci.*, 24(1), 208–216. https://doi.org/10.1016/j.sjbs.2016.02.025
39. Eskandari-Nojedehi, M., Jafarizadeh-Malmiri, H. & Rahbar-Shahrouzi, J. (2018). Hydrothermal green synthesis of gold nanoparticles using mushroom (*Agaricus bisporus*) extract: Physico-chemical characteristics and antifungal activity studies. *Green Process. Synth.*, 7(1), 38–47. https://doi.org/10.1515/gps-2017-0004
40. Patra, J. K. & Baek, K.-H. (2016). Comparative study of proteasome inhibitory, synergistic antibacterial, synergistic anticandidal, and antioxidant activities of gold nanoparticles biosynthesized using fruit waste materials. *Int. J. Nanomed.*, 11, 4691–4705. https://doi.org/10.2147/IJN.S108920
41. Acisli, O. et al. (2017). Ultrasound-assisted Fenton process using siderite nanoparticles prepared via planetary ball milling for removal of reactive yellow 81 in aqueous phase. *Ultrason. Sonochem.*, 35, 210–218. https://doi.org/10.1016/j.ultsonch.2016.09.020
42. Braim, F. S. et al. (2023). Rapid green-assisted synthesis and functionalization of superparamagnetic magnetite nanoparticles using sumac extract and assessment of their cellular toxicity, uptake, and anti-metastasis property. *Ceram. Int.*, 49(5), 7359–7369. https://doi.org/10.1016/j.ceramint.2022.10.207
43. Jameel, M. S. et al. (2020). Rapid sonochemically-assisted green synthesis of highly stable and biocompatible platinum nanoparticles. *Surf. Interfaces*, 20, 100635. https://doi.org/10.1016/j.surfin.2020.100635
44. Xiong, B. et al. (2025). Effects of dark treatment on 'Yinhongli' plum phenolic biosynthesis and antioxidant capacity analysed through transcriptomic and metabolomic approaches. *Sci. Hortic.*, 349, 114233. https://doi.org/10.1016/j.scienta.2025.114233

45. Michalska, A. et al. (2017). Chemical composition and antioxidant properties of powders obtained from different plum juice formulations. *Int. J. Mol. Sci.*, 18(1), 176. https://doi.org/10.3390/ijms18010176
46. Tepale, N. et al. (2019). Nanoengineering of gold nanoparticles: Green synthesis, characterization, and applications. *Crystals*, 9(12), 612. https://doi.org/10.3390/cryst9120612
47. Shafiqa, A., Aziz, A. A. & Mehrdel, B. (2018). Nanoparticle optical properties: Size dependence of a single gold spherical nanoparticle. *J. Phys. Conf. Ser.*, 012040. https://doi.org/10.1088/1742-6596/1083/1/012040
48. Rabeea, M. A. et al. (2020). Mycosynthesis of gold nanoparticles using the extract of *Flammulina velutipes*, Physalacriaceae, and their efficacy for decolorization of methylene blue. *J. Environ. Chem. Eng.*, 8(3), 103841. https://doi.org/10.1016/j.jece.2020.103841
49. Khaniabadi, P. M. et al. (2021). Structure, morphology and absorption characteristics of gold nanoparticles produced via PLAL method: Role of low energy X-ray dosage. *Surf. Interfaces*, 24, 101139. https://doi.org/10.1016/j.surfin.2021.101139
50. Amendola, V., Pilot, R., Frasconi, M., Maragò, O. M. & Iatì, M. A. (2017). Surface plasmon resonance in gold nanoparticles: A review. *J. Phys. Condens. Matter*, 29(20), 203002. https://doi.org/10.1088/1361-648X/aa60f3
51. Keskin, C. et al. (2022). Green synthesis, characterization of gold nanomaterials using *Gundelia tournefortii* leaf extract, and determination of their nanomedicinal potential. *J. Nanomater.*, 2022, 1–12. https://doi.org/10.1155/2022/7211066
52. Radaic, A. et al. (2021). Phosphatidylserine-gold nanoparticles (PS-AuNP) induce prostate and breast cancer cell apoptosis. *Pharma.*, 13(7), 1094. https://doi.org/10.3390/pharmaceutics13071094
53. Sanati, M. et al. (2022). Recent trends in the application of nanoparticles in cancer therapy: The involvement of oxidative stress. *J. Control. Release*, 348, 287–304. https://doi.org/10.1016/j.jconrel.2022.05.035
54. Gallud, A. et al. (2019). Cationic gold nanoparticles elicit mitochondrial dysfunction: A multi-omics study. *Sci. Rep.*, 9(1), 4366. https://doi.org/10.1038/s41598-019-40579-6
55. Lin, J. et al. (2010). Penetration of lipid membranes by gold nanoparticles: Insights into cellular uptake, cytotoxicity, and their relationship. *ACS Nano*, 4(9), 5421–5429. https://doi.org/10.1021/nn1010792
56. Yadav, M. et al. (2021). Targeting nonapoptotic pathways with functionalized nanoparticles for cancer therapy: Current and future perspectives. *Nanomed.*, 16(12), 1049–1065. https://doi.org/10.2217/nnm-2020-0443
57. Dheyab, M. A. et al. (2024). Recent advances of plant-mediated metal nanoparticles: Synthesis, properties, and emerging applications for wastewater treatment. *J. Environ. Chem. Eng.*, 112345. https://doi.org/10.1016/j.jece.2024.112345
58. Dheyab, M. A. et al. (2023). Exploring the anticancer potential of biogenic inorganic gold nanoparticles synthesized via mushroom-assisted green route. *Inorg. Chem. Commun.*, 157, 111363. https://doi.org/10.1016/j.inoche.2023.111363

59. Omran, H. J. et al. (2025). Extraction, characterization, and biological activities of anthocyanin pigment from *Prunus domestica* L. fruit peels. *Cogent. Food Agric.*, 11(1), 2484362. https://doi.org/10.1080/23311932.2025.2484362
60. Sudhakaran, M. & Doseff, A. I. (2020). The targeted impact of flavones on obesity-induced inflammation and the potential synergistic role in cancer and the gut microbiota. *Molecules*, 25(11), 2477. https://doi.org/10.3390/molecules25112477
61. Anand, K. et al. (2015). Agroforestry waste *Moringa oleifera* petals mediated green synthesis of gold nanoparticles and their anti-cancer and catalytic activity. *J. Ind. Eng. Chem.*, 21, 1105–1111. https://doi.org/10.1016/j.jiec.2014.05.021
62. Pechyen, C. et al. (2021). Waste fruit peel–mediated green synthesis of biocompatible gold nanoparticles. *J. Mater. Res. Technol.*, 14, 2982–2991. https://doi.org/10.1016/j.jmrt.2021.08.111
63. Gubitosa, J. et al. (2022). The "end life" of the grape pomace waste become the new beginning: The development of a virtuous cycle for the green synthesis of gold nanoparticles and removal of emerging contaminants from water. *Antioxidants*, 11(5), 994. https://doi.org/10.3390/antiox11050994
64. Ngungeni, Y. et al. (2023). Anticancer, antioxidant, and catalytic activities of green synthesized gold nanoparticles using avocado seed aqueous extract. *ACS Omega*, 8(29), 26088–26101. https://doi.org/10.1021/acsomega.3c02260
65. Akintelu, S. A., Yao, B. & Folorunso, A. S. (2021). Green synthesis, characterization, and antibacterial investigation of synthesized gold nanoparticles (AuNPs) from *Garcinia kola* pulp extract. *Plasmonics*, 16(1), 157–165. https://doi.org/10.1007/s11468-020-01274-9